Photonic-to-plasmonic mode converter

Argishti Melikyan,[1,2,*] Manfred Kohl,[1] Martin Sommer,[1] Christian Koos,[1,2] Wolfgang Freude,[1] and Juerg Leuthold[1,2,3]

[1]*Insitute of Microstructure Technology, Karlsruhe Institute of Technology, 76344 Eggenstein-Leopoldshafen, Germany*

[2]*Insitute of Photonics and Quantum Electronics, Karlsruhe Institute of Technology, 76131 Karlsruhe, Germany*

[3]*Institute of Electromagnetic Fields (IEF), ETH Zurich, 8092 Zurich, Switzerland*

**Corresponding author: argishti.melikyan@kit.edu*

Received March 5, 2014; revised May 4, 2014; accepted May 5, 2014;
posted May 7, 2014 (Doc. ID 207655); published June 6, 2014

A novel photonic-to-plasmonic mode converter for efficiently converting a silicon strip waveguide mode to a gap surface plasmon polariton (SPP) of a metallic slot structure is proposed. A conversion efficiency of more than 85% is found for metallic slots with a slot size of 30–50 nm. Calculations show that high conversion efficiencies can be achieved for various cladding materials with refractive indices of 1.44, 1.6, and 1.7. The optical 1 dB bandwidth of the converter is around 200 nm. The proposed mode converter shows a good tolerance with respect to fabrication errors, and it requires a simple fabrication procedure only. © 2014 Optical Society of America

OCIS codes: (250.5403) Plasmonics; (230.2090) Electro-optical devices; (250.4110) Modulators.
http://dx.doi.org/10.1364/OL.39.003488

Surface plasmon polaritons (SPPs) are key to a new generation of plasmonic integrated circuits (ICs) with dimensions that are compatible with electronic IC sizes [1,2]. The high optical loss originating in metals, however, is a bottleneck for plasmonics. A typical 0.5 dB/μm propagation loss of a SPP [3] confines their application range to ultrashorrt components only. To solve this issue, the combination of compact plasmonic active components such as modulators, switches, phase shifters, and lasers with other low-loss silicon photonic strip waveguides (WGs) seems to be attractive and might lead to new ICs comprising SPP devices, photonic circuits, and electronics [4]. The merging of plasmonics and low-loss silicon photonics, however, calls for an efficient coupling scheme.

A basic plasmonic building block that can easily be cointegrated with electronic ICs is the metallic slot waveguide (MSW) [5–9]. Such MSWs can confine light to sub-100-nm slots resulting in so-called gap SPPs. Gap SPPs exhibit extremely small penetration depths both in the substrate and the cladding. Devices comprising MSWs can be placed a few micrometers apart, thereby significantly increasing the integration density of optical components. In addition, the two metallic guides are very practical for electrically connecting active devices such as plasmonic photodetectors [10], light sources [11,12], and modulators [13–23]. Two configurations of MSWs have been reported [8] with either vertically [5–9] or horizontally [24] orientated slots as shown in Fig. 1(a) and Fig. 1(b), respectively. When MSW structures are used as modulators, it is of particular importance that the separation h between the metals is designed to be small, i.e., below 100 nm, and that the width w is larger than 150 nm for achieving a strong field enhancement in the slot. However, fabrication of a metallic slot in Fig. 1(a) with a large w/h aspect ratio as well as excitation of its gap SPP becomes challenging. While several methods have been reported to excite the gap SPP in vertical MSWs [25–31], fabrication of high aspect ratio slots in a vertical configuration is still a major issue. Alternatively, the horizontal MSWs of Fig. 1(b) can more easily be fabricated with a large aspect ratio by means of a bottom-up approach. However, so far, the proposed approaches to excite the gap SPP in the horizontal MSW require a highly accurate lithography step and do not provide easy control over the coupling efficiency [24].

In this Letter, we propose a novel coupling scheme between a silicon strip WG and a horizontal MSW with a conversion efficiency of more than 85% over a broad band of optical frequencies. Particularly, we show that a photonic mode of the silicon strip WG can be fully converted into a gap SPP of a sub-50-nm metallic slot filled with an insulator material having refractive indices of 1.44, 1.6, and 1.7. We also discuss the influence of various fabrication errors on the coupler performance. The proposed converter can be used in various plasmonic devices where an efficient and controllable excitation and extraction of the gap SPP is needed.

The operation principle of the proposed mode converter is based on ideas similar to the ones underlying directional couplers and multimode interference (MMI) couplers; see Fig. 2 [32]. A photonic mode propagating through a silicon WG with a height of 340 nm and a width of 300 nm excites supermodes in the photonic-plasmonic MMI-like coupling section (CS) of length L. By properly selecting the length L and other geometrical parameters, a gap SPP can efficiently be excited in the end of the CS. Depending on the application, the silicon WG can either be terminated after the CS or extended beyond this point.

We optimize the device's performance at the wavelength of 1.55 μm employing the simplified eigenmode expansion (EME) [33] method. To find the coupling strength of arbitrary eigenmodes i and j, we use the general orthogonality relation [34]

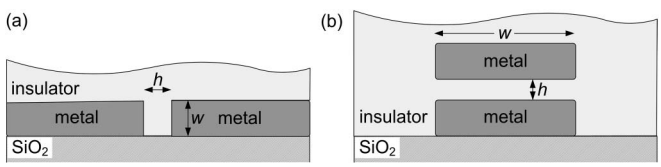

Fig. 1. Metallic slot WGs in two different configurations. (a) Vertically oriented and (b) horizontally oriented MSWs.

 © 2014 Optical Society of America

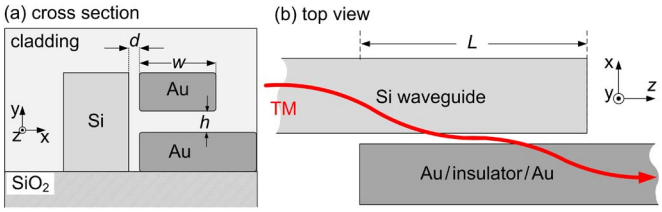

Fig. 2. (a) Cross-section and (b) top view of the suggested coupler. The TM mode launched into the silicon strip WG couples to a plasmonic WG via a CS of length L.

$$\underbrace{\frac{1}{4}\iint [\mathbf{e}_i \times \mathbf{h}_j + \mathbf{h}_i \times \mathbf{e}_j]_z \mathrm{d}x\mathrm{d}y}_{C^{ij}} = \delta_{ij}\underbrace{\frac{1}{2}\iint [\mathbf{e}_i \times \mathbf{h}_j]_z \mathrm{d}x\mathrm{d}y}_{P_{ij}}, \quad (1)$$

Thus, the normalized overlap integral between modes i and j can be written as

$$c_i^j = \frac{C^{ij}}{\sqrt{P_{ii}P_{jj}}}. \quad (2)$$

Neglecting backward propagating waves, we study light propagation in the CS as a superposition of all supermodes, including guiding, leaky, and radiating modes. The distributions of the electric $\mathbf{E}_{\mathrm{CS}}(x,y,z)$ and the magnetic fields $\mathbf{H}_{\mathrm{CS}}(x,y,z)$ in the CS can be written as

$$\mathbf{E}_{\mathrm{CS}}(x,y,z) = \sum_{\mu=1}^{N} c_\mu^s \mathbf{e}_\mu(x,y) \cdot e^{-j\beta_\mu z},$$
$$\mathbf{H}_{\mathrm{CS}}(x,y,z) = \sum_{\mu=1}^{N} c_\mu^s \mathbf{h}_\mu(x,y) \cdot e^{-j\beta_\mu z}. \quad (3)$$

Here, the indices μ and s stand for supermode and silicon strip WG photonic modes, respectively. The quantities $\mathbf{e}_\mu(x,y)$ and $\mathbf{h}_\mu(x,y)$ are the electric and the magnetic fields of the μth supermode. The complex propagation constant (which includes losses) and the excitation efficiency of the μth supermode are defined as β_μ and c_μ^s, respectively. The excitation efficiency c_μ^s is calculated as an overlap integral Eq. (2) between the silicon WG photonic mode and a specific supermode μth. An example of the electric field distribution in a CS with a length of 5 μm is given in Fig. 3(a) for a MSW with a width w of 200 nm, a slot height h of 60 nm, and a distance d of 20 nm.

The supermodes of the CS are simulated with the finite element method (FEM) [35]. To estimate the final photonic-to-plasmonic mode conversion efficiency, first the gap SPP is independently simulated for a homogenous cladding, and then the distributions of the electric $\mathbf{e}_{\mathrm{MSW}}(x,y)$ and the magnetic field $\mathbf{h}_{\mathrm{MSW}}(x,y)$ are calculated. The final conversion efficiency is computed as a normalized overlap integral $c_{\mathrm{MSW}}^{\mathrm{CS}}(z)$ of the gap SPP with the field distributions at the CS $\mathbf{E}_{\mathrm{CS}}(x,y,z)$ and $\mathbf{H}_{\mathrm{CS}}(x,y,z)$.

Figure 3(b) shows the magnitude of the overlap integral $|c_{\mathrm{MSW}}^{\mathrm{CS}}(z)|$ versus the z-coordinate for a distance d of 20 nm (red) and 60 nm (black). The maximum value

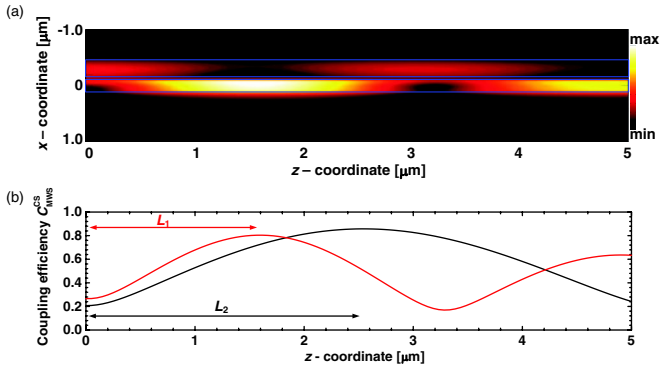

Fig. 3. Electric field distribution and optimum length of the mode converter. (a) Color-coded plot of the y-component of an electric field magnitude referring to subfigure (b), red curve. (b) Coupling efficiency as a function of converter length. Two different distances d of 20 nm (red) and 60 nm (black) lead to different converter lengths L_1 and L_2. The mode converter has a width w of 200 nm, a slot height of h of 60 nm, and an organic cladding with a refractive index of 1.7.

of $|c_{\mathrm{MSW}}^{\mathrm{CS}}(z)|$ is taken as the best conversion efficiency, and the corresponding z-coordinate is the respective optimum CS length $L_{1,2}$. As can be seen, the distance d mainly influences the coupling length L. The larger the distance d, the longer the coupling length L becomes.

The conversion efficiency and the coupling length are given in Fig. 4 as a function of the distance d and the slot height h for MSWs with a width w of 200 nm and for various cladding materials. Glass with a refractive index of 1.44 is shown in Figs. 4(a) and 4(b), organic materials with refractive indices of 1.6 are shown in Fig. 4(c) and 4(d), and materials with indices of 1.7 are shown in Figs. 4(e) and 4(f). For all three types of cladding materials, a maximum conversion efficiency of 85% can be achieved for MSWs with sub-50-nm slots. This can be achieved using an optimum CS length of $L = 1.4\ldots2$ μm and a distance d of 20…60 nm. In experimentally defining a distance d it is mainly the fabrication alignment precision that matters, and this not a fundamental problem with modern DUV and e-beam lithographical systems. Moreover, by varying geometrical parameters, e.g., the distance d, the conversion, efficiency can be tuned. This might be needed, e.g., in the case of plasmonic lasers where a well-defined outcoupling of power from the resonator is required. The proposed coupling scheme shows great tolerance with respect to fabrication errors, which can affect the final length L. Additionally, the variation in conversion efficiency, associated with errors of ±20 nm in defining the distance d, is below 5%.

Furthermore, we study the influence of the MSW width w on the device performance. The conversion efficiency and the CS length as calculated for a 300 nm wide MSW with a cladding refractive index of 1.7 are given in Fig. 5(a) and Fig. 5(b), respectively. A conversion efficiency of 80% can be achieved for a metallic slot with a height of 50 nm, i.e., for a MSW with an aspect ratio of 6. MSW with such a large aspect ratio are difficult to realize in a vertical configuration, whereas in the horizontal configuration they can easily be fabricated.

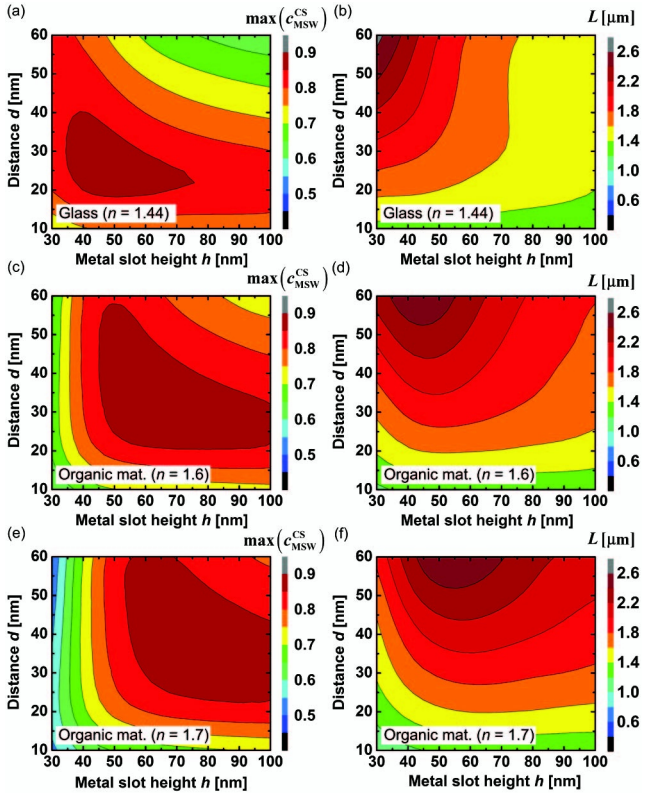

Fig. 4. (a), (c), (e) Conversion efficiency and (b), (d), (f) optimum CS length L for a horizontal MSW with a width w of 200 nm and for various cladding materials: (a) and (b) for glass with a refractive index of 1.44, (c) and (d) for organic materials with refractive indices of 1.6, and (e) and (f) for refractive index of 1.7.

To investigate how the performance of the proposed mode converter depends on the carrier wavelength, we numerically investigate the mode conversion mechanism in a converter with a glass cladding ($n = 1.44$) using a finite-difference time-domain (FDTD) method. A metallic slot height h of 30 nm and a distance d of 60 nm are chosen. To obtain an optimum operation for a wavelength of 1.55 μm, we select a CS length of $L = 2.6$ μm, based on data given in Figs. 4(a)–4(b). The computed transmission and reflection spectra are given in Fig. 6(a). The wavelength dependence of the optical properties of Au is taken into account by an appropriate Drude model. No strong resonance behavior is seen in

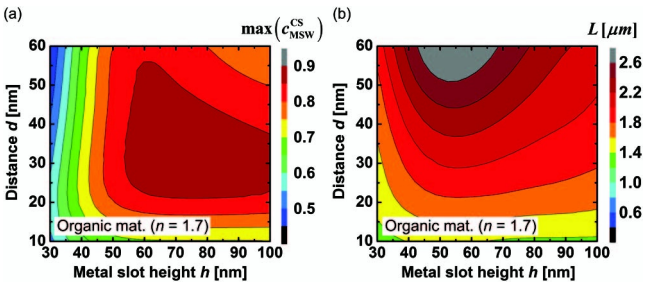

Fig. 5. Conversion efficiency and coupling length for a horizontal MSW with a width w of 300 nm and a cladding refractive index of 1.7. (a) Conversion efficiency and (b) coupling length for various distances d and slot sizes h.

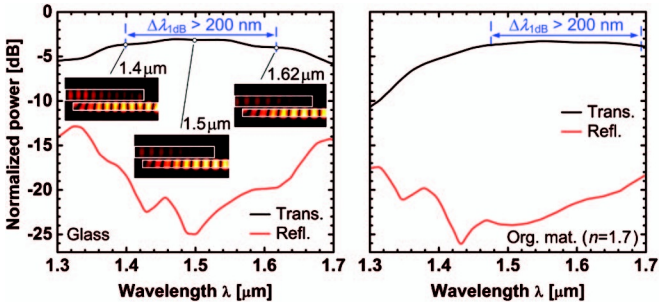

Fig. 6. Transmission (black) and reflection spectra (red) of the mode converter for a glass and an organic cladding. The Si nanowire in front of the coupling zone defines the input port, the MSW after the coupling zone represents the output port. Operating 1 dB bandwidth of the converter is in the range of 200 nm for both cladding materials. (a) Glass. Transmission and reflection spectra for a converter having a height h of 30 nm, a distance d of 60 nm, a CS length L of 2.6 μm and a cladding material with a refractive index of 1.44. In addition, the electric field distributions at carrier wavelengths of 1.4, 1.5, and 1.62 μm are given as insets. (b) Organic material. Transmission and reflection spectra for a converter having a height h of 60 nm, a distance d of 60 nm, a CS length L of 2.5 μm, and a cladding material with a refractive index of 1.7.

the optical response of the mode converter. The transmission and reflection spectra of a mode converter with a slot height h of 60 nm and a distance d of 60 nm are given in Fig. 6(b) for an organic cladding ($n = 1.7$). For an optimum operation, we select the CS length L to be 2.5 μm. For both cladding materials, the 1 dB bandwidth of the proposed device is in the range of 200 nm, which is comparable to the one reported for metallic taper mode converters [29]. At the central wavelength 1.55 μm, the photonic-to-plasmonic coupling loss is about 3 dB, which includes propagation losses in the CS with a length of L and in the MSW with a length of 0.5 μm.

To conclude, we report on a novel photonic-to-plasmonic mode converter for silicon photonics. The approach provides more than 85% conversion efficiency for a gap SPP in a horizontal MSW, where the sub-50-nm slot is filled with various insulator materials. The proposed mode converter does not exhibit any resonant behavior and can be operated in a wide wavelength range. It requires only a simple "bottom-up" fabrication approach and shows good tolerance with respect to fabrication errors.

The authors acknowledge support from the EU-funded project NAVOLCHI, the Helmholtz International Research School for Teratronics (HIRST), the Karlsruhe School of Optics & Photonics (KSOP), the Center for Functional Nanostructures (CFN), and the German Research Foundation (DFG).

References

1. H. Raether, *Surface Plasmons on Smooth and Rough Surfaces and on Gratings* (Springer, 1988).
2. D. K. Gramotnev and S. I. Bozhevolnyi, Nat. Photonics **4**, 83 (2010).
3. S. Zhu, T. Y. Liow, G. Q. Lo, and D. L. Kwong, Opt. Express **19**, 8888 (2011).
4. S. Papaioannou, D. Kalavrouziotis, K. Vyrsokinos, J.-C. Weeber, K. Hassan, L. Markey, A. Dereux, A. Kumar,

S. I. Bozhevolnyi, M. Baus, T. Tekin, D. Apostolopoulos, H. Avramopoulos, and N. Pleros, Sci. Rep. **2**, 1 (2012).
5. B. Prade, J. Y. Vinet, and A. Mysyrowicz, Phys. Rev. B **44**, 13556 (1991).
6. D. F. P. Pile, D. K. Gramotnev, R. F. Oulton, and X. Zhang, Opt. Express **15**, 13669 (2007).
7. N. Feng, M. L. Brongersma, and L. D. Negro, IEEE J. Quantum Electron. **43**, 479 (2007).
8. G. Veronis and S. Fan, J. Lightwave Technol. **25**, 2511 (2007).
9. J. A. Dionne, L. A. Sweatlock, M. T. Sheldon, A. P. Alivisatos, and H. A. Atwater, IEEE J. Sel. Top. Quantum Electron. **16**, 295 (2010).
10. S. Zhu, G. Q. Lo, and D. L. Kwong, Opt. Express **19**, 15843 (2011).
11. Y. C. Jun, R. D. Kekatpure, J. S. White, and M. L. Brongersma, Phys. Rev. B **78**, 153111 (2008).
12. K. C. Y. Huang, M.-K. Seo, T. Sarmiento, Y. Huo, J. S. Harris, and M. L. Brongersma, Nat. Photonics **8**, 244 (2014).
13. J. S. Schildkraut, Appl. Opt. **27**, 4587 (1988).
14. W. Cai, J. S. White, and M. L. Brongersma, Nano Lett. **9**, 4403 (2009).
15. S. Randhawa, S. Lachèze, J. Renger, A. Bouhelier, R. E. de Lamaestre, A. Dereux, and R. Quidant, Opt. Express **20**, 2354 (2012).
16. M. Xu, F. Li, T. Wang, J. Wu, L. Lu, L. Zhou, and Y. Su, J. Lightwave Technol. **31**, 1170 (2013).
17. A. Melikyan, L. Alloatti, A. Muslija, D. Hillerkuss, P. C. Schindler, J. Li, R. Palmer, D. Korn, S. Muehlbrandt, D. Van Thourhout, B. Chen, R. Dinu, M. Sommer, C. Koos, M. Kohl, W. Freude, and J. Leuthold, Nat. Photonics **8**, 229 (2014).
18. J. A. Dionne, K. Diest, L. A. Sweatlock, and H. A. Atwater, Nano Lett. **9**, 897 (2009).
19. S. Zhu, G. Q. Lo, and D. L. Kwong, Opt. Express **18**, 27802 (2010).
20. E. Feigenbaum, K. Diest, and H. A. Atwater, Nano Lett. **10**, 2111 (2010).
21. V. J. Sorger, N. D. Lanzillotti-Kimura, R.-M. Ma, and X. Zhang, J. Nanophoton. **1**, 17 (2012).
22. A. Melikyan, N. Lindenmann, S. Walheim, P. M. Leufke, S. Ulrich, J. Ye, P. Vincze, H. Hahn, T. Schimmel, C. Koos, W. Freude, and J. Leuthold, Opt. Express **19**, 8855 (2011).
23. V. E. Babicheva and A. V. Lavrinenko, Opt. Commun. **285**, 5500 (2012).
24. R. Yang and Z. Lu, IEEE Photon. Technol. Lett. **23**, 1652 (2011).
25. D. F. P. Pile and D. K. Gramotnev, Appl. Phys. Lett. **89**, 041111 (2006).
26. C. Delacour, S. Blaize, P. Grosse, J. M. Fedeli, A. Bruyant, R. Salas-Montiel, G. Lerondel, and A. Chelnokov, Nano Lett. **10**, 2922 (2010).
27. G. Veronis and S. Fan, Opt. Express **15**, 1211 (2007).
28. A. Kriesch, S. P. Burgos, D. Ploss, H. Pfeifer, H. A. Atwater, and U. Peschel, Nano Lett. **13**, 4539 (2013).
29. J. Tian, S. Yu, W. Yan, and M. Qiu, Appl. Phys. Lett. **95**, 013504 (2009).
30. L. Chen, J. Shakya, and M. Lipson, Opt. Lett. **31**, 2133 (2006).
31. O. Tsilipakos, A. Pitilakis, T. V. Yioultsis, S. Papaioannou, K. Vyrsokinos, D. Kalavrouziotis, G. Giannoulis, D. Apostolopoulos, H. Avramopoulos, T. Tekin, M. Baus, M. Karl, K. Hassan, J.-C. Weeber, L. Markey, A. Dereux, A. Kumar, S. I. Bozhevolnyi, N. Pleros, and E. E. Kriezis, IEEE J. Quantum Electron. **48**, 678 (2012).
32. J. Leuthold, J. Eckner, E. Gamper, P. A. Besse, and H. Melchior, J. Lightwave Technol. **16**, 1228 (1998).
33. D. F. G. Gallagher and T. P. Felici, Proc. SPIE **4987**, 69 (2003).
34. A. W. Snyder, *Optical Waveguide Theory* (Chapman & Hall, 1983).
35. www.comsol.com.